Article

Hypertrophy and Unconventional Cell Division of Hepatocytes Underlie Liver Regeneration

Yuichiro Miyaoka,[1] Kazuki Ebato,[1] Hidenori Kato,[1]
Satoko Arakawa,[2] Shigeomi Shimizu,[2]
and Atsushi Miyajima[1,*]
[1]Laboratory of Cell Growth and Differentiation, Institute of
Molecular and Cellular Biosciences, The University of Tokyo,
Yayoi, Bunkyo-ku, Tokyo 113-0032, Japan
[2]Department of Pathological Cell Biology, Medical Research
Institute, Tokyo Medical and Dental University, Yushima,
Bunkyo-ku, Tokyo 113-8510, Japan

Summary

Background: The size of organs and tissues is basically determined by the number and size of their cells. However, little attention has been paid to this fundamental concept. The liver has a remarkable ability to regenerate after surgical resection (partial hepatectomy [PHx]), and hepatocytes account for about 80% of liver weight, so we investigate how the number and size of hepatocytes contribute to liver regeneration in mice. It has been generally accepted that hepatocytes undergo one or two rounds of cell division after 70% PHx. However, ploidy of hepatocytes is known to increase during regeneration, suggesting an unconventional cell cycle. We therefore examine cell cycle of hepatocytes in detail.
Results: By developing a method for genetic fate mapping and a high-throughput imaging system of individual hepatocytes, we show that cellular hypertrophy makes the first contribution to liver regeneration; i.e., regeneration after 30% PHx is achieved solely by hypertrophy without cell division, and hypertrophy precedes proliferation after 70% PHx. Proliferation and hypertrophy almost equally contribute to regeneration after 70% PHx. Furthermore, although most hepatocytes enter cell cycle after 70% PHx, not all hepatocytes undergo cell division. In addition, binuclear hepatocytes undergo reductive divisions to generate two mononuclear daughter hepatocytes in some cases.
Conclusions: Our findings demonstrate the importance of hypertrophy and the unconventional cell division cycle of hepatocytes in regeneration, prompting a significant revision of the generally accepted model of liver regeneration.

Introduction

How the size of organs and tissues is regulated in development and regeneration is a fundamental question in biology [1, 2]. Fankhauser's historical observation of salamanders with a different ploidy demonstrated that cell numbers are inversely correlated with cell size and ploidy, allowing the organ size to remain the same [3]. A similar observation was made in tetraploid mouse embryos [4]. In the *Drosophila* wing, cells undergo atrophy/hypertrophy to compensate for changes in cell number to maintain the size of imaginal discs [5]. Furthermore, it has been demonstrated that the difference in the size of an organ in various mammals is mainly due to cell number,

not cell size [6]. These are a few examples of studies showing the relation between organ size and the number and size of cells comprising the organ. However, not much attention has been paid to how cell size and number contribute to organ size in development and regeneration.

The liver has a remarkable capacity to regenerate. Even when 70% of its mass is surgically removed, the remnant tissue expands to compensate for the lost tissue and functions [7, 8]. The multilobular structure of rodent livers allows the surgical resection of a lobe of choice to achieve different levels of loss of liver mass by partial hepatectomy (PHx). Because the resection of lobes does not induce damage to the remaining tissue, PHx is a clean model. Therefore, liver regeneration after PHx has long been an excellent experimental model for tissue regeneration. Furthermore, although the liver consists of various types of cells, hepatocytes account for about 80% of liver weight and about 70% of all liver cells [9]. Thus, hepatocytes provide an ideal model to study the relation of organ size with number and size of cells.

It has been generally accepted that liver regeneration depends mainly on the proliferation of hepatocytes [7, 8, 10, 11]. In the simplest model without considering the possible change of cell size, all hepatocytes are expected to divide about 1.6 times after 70% PHx. However, there are several reports showing hypertrophy of hepatocytes in the regenerated liver [12–14] and it has not been investigated how the proliferation and hypertrophy of hepatocytes contribute to liver regeneration. Previous studies using the uptake of tritiated-thymidine showed that at least 84% of hepatocytes enter into S phase during liver regeneration [15]. However, entry into S phase does not necessarily mean cell division. Moreover, it is known that the ploidy of hepatocytes increases in the regenerated liver, suggesting that S phase is not always followed by a normal M phase [14, 16]. In addition, adult liver has many binuclear hepatocytes and the number of binuclear hepatocytes decreases during the regeneration [17]. These observations suggest that the cell division cycle of hepatocytes in regenerating liver may not follow normal processes. However, conventional analyses using bulk hepatocytes do not provide sufficient information as to the mechanism underlying such unique features of hepatocyte proliferation during regeneration.

To revisit the fundamental questions on the contribution of the size and number of hepatocytes to regeneration after PHx, we have developed two novel systems. One is an unbiased high-throughput system using an imaging cytometer to evaluate cell and nuclear size, number of nuclei, and expression of cell cycle markers in a large number of hepatocytes at the same time. The other is a genetic tracing system that marks individual cells permanently and randomly using transient expression of Cre recombinase by hydrodynamic tail vein injection (HTVi) [18], which allows the evaluation of cell division at the single-cell level. The imaging cytometric analysis revealed that the size of hepatocytes increases significantly, and hypertrophy and proliferation almost equally contribute to the regeneration after 70% PHx. Regeneration after 30% PHx and the initial phase of the regenerative process after 70% PHx depend solely on hypertrophy but not proliferation. Surprisingly, genetic tracing experiments showed that

*Correspondence: miyajima@iam.u-tokyo.ac.jp

A

Normal liver   Day 0   70% PHx Day 14

B

C   Sham Day 2   Day 0   70% PHx Day 1   70% PHx Day 2   70% PHx Day 3

Ki67/Nucleus

70% PHx Day 4   70% PHx Day 5   70% PHx Day 6   70% PHx Day 7   70% PHx Day 14
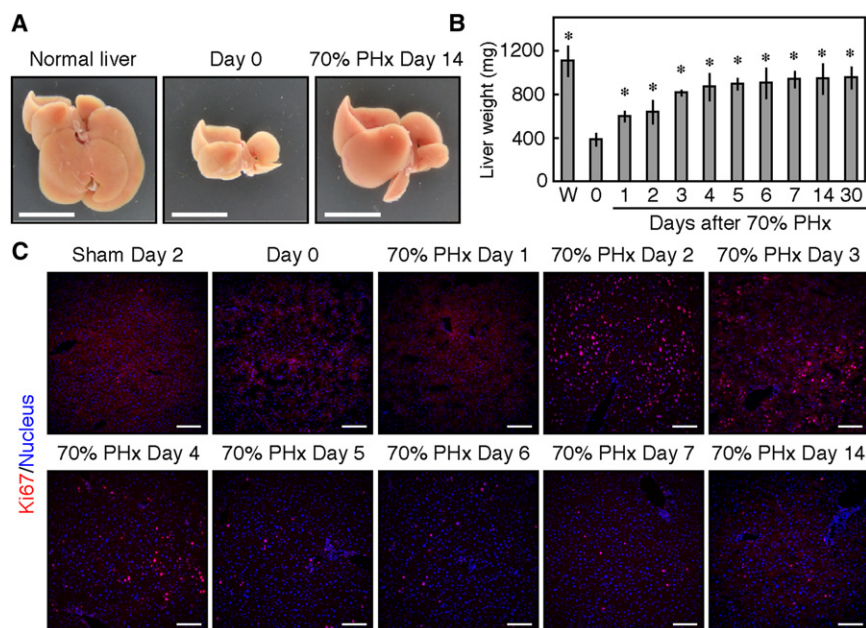
Figure 1. Liver Regeneration after 70% PHx

(A) Liver regeneration. The median and left lobes were surgically removed in 70% PHx. The remaining tissue expanded in mass by 14 days after 70% PHx. Scale bars represent 1 cm.

(B) Changes of liver weight during liver regeneration. p value between each time point and day 0 was calculated by Student's t test (*p < 0.001). Error bars represent SD. W, whole liver before PHx.

(C) Time course of entry into cell cycle of hepatocytes during liver regeneration. Immunofluorescent staining of Ki67 (red) was performed on liver sections at each time point after 70% PHx. Nuclei (blue) were stained with Hoechst33342. Note that at 1 day after 70% PHx, very few cells were Ki67^{+}, whereas the liver weight significantly increased. Quantification of Ki67^{+} hepatocytes is shown in Figure S5E. Scale bars represent 100 μm.

only about half of hepatocytes undergo cell division during regeneration after 70% PHx. Moreover, we found that binuclear hepatocytes undergo reductive cell divisions to generate two mononuclear daughter hepatocytes and revealed unconventional cell cycle progression of hepatocytes during liver regeneration. In this paper, we provide various lines of evidence showing unique features of hepatocytes in regeneration, which require a significant revision of the generally accepted view of liver regeneration.

Results

Liver Weight Increases without Proliferation of Hepatocytes at the Early Phase of Liver Regeneration

In mice, liver weight increased from 1 day after 70% PHx and reached a plateau by 7 days as reported previously (Figures 1A and 1B) [7]. The remaining liver lobes increased about 2.4-fold in weight during the regeneration (Figure 1B). TUNEL assays showed no obvious apoptosis throughout the regenerative processes (Figure S1 available online) as shown previously [19], excluding the effects of apoptosis on the number of hepatocytes. Immunofluorescent staining of Ki67, which is expressed from the G1 to M phase but not in the G0 phase, clearly showed that hepatocytes vigorously entered the cell cycle at 2 days after 70% PHx, but the number of Ki67^{+} cells dropped at 3 days after 70% PHx (Figure 1C). We quantified the proportion of Ki67^{+} hepatocytes and found that it was less than 1% and about 49% at 1 and 2 days after 70% PHx, respectively (see below and Figures S5B and S5E). Interestingly, although there were few Ki67^{+} hepatocytes at 1 day after 70% PHx, liver weight had increased considerably by that time (Figures 1B and 1C). These results indicated that the proliferation of hepatocytes alone could not account for the recovery of liver mass after 70% PHx. Therefore, we investigated the size of hepatocytes during liver regeneration.

Hepatocytes Enlarge during Liver Regeneration

To investigate the size of hepatocytes, we developed a new imaging cytometric approach. Because hepatocytes are

epithelial cells, their outlines can be visualized by actin staining (Figure 2A). The cytometer recognizes nuclei with a certain roundness at first and then the surrounding actin signals as the outline of a cell, allowing an estimation of cell size. Because hepatocytes are much larger than other cell types, they can be distinguished based on size. This procedure also recognizes both mononuclear and binuclear hepatocytes (Figure 2A) and allows us to scan a large number of hepatocytes in a liver section efficiently and thoroughly (Figure 2B). Then, we measured the area of each hepatocyte during liver regeneration and found an increase in size at 1 and 7 days after 70% PHx (Figure 2C). Quantitative analysis revealed that the size of hepatocytes had increased slightly as early as 3 hr after 70% PHx, peaked at 1 day after 70% PHx, and then gradually decreased (Figure 2D). Because the hepatocytes were significantly larger at 14 days after 70% PHx than the sham operation control, hypertrophy of hepatocytes was maintained even after the recovery of liver weight (Figure 2D). Although this tendency was maintained even at 30 days after 70% PHx, it was not statistically significant (Figure 2D). Therefore, we performed most experiments within 14 days after 70% PHx hereafter. We also found that the nuclei enlarged during regeneration, suggesting increased DNA content per nucleus (Figures 2C and 2E). However, nuclear hypertrophy does not seem to be a direct cause of cellular hypertrophy, because cellular hypertrophy precedes it (Figures 2C–2E). We converted the data on area and concluded that hepatocytes increased in volume by 2.0-fold and 1.5-fold at 1 and 14 days after 70% PHx, respectively (Figure 2F). These results provide quantitative evidence, for the first time, that not only the proliferation but also the hypertrophy of hepatocytes significantly contributes to liver regeneration. Notably, the early phase of liver regeneration is largely dependent on the hypertrophy of hepatocytes, because the increase in liver weight 1 day after 70% PHx matched the increase in hepatocyte size (Figures 1B and 2F). It is known that lipids accumulate in hepatocytes immediately after 70% PHx [20]. Consistently, oil-red O staining and electron microscopy revealed intensive lipid accumulation 1 day after 70% PHx (Figures S2A and S2B). However, these lipids disappeared by 14 days after 70% PHx (Figure S2B), indicating that the lipids accounted for, at least in part, the rapid increase in hepatocyte size after 70% PHx,
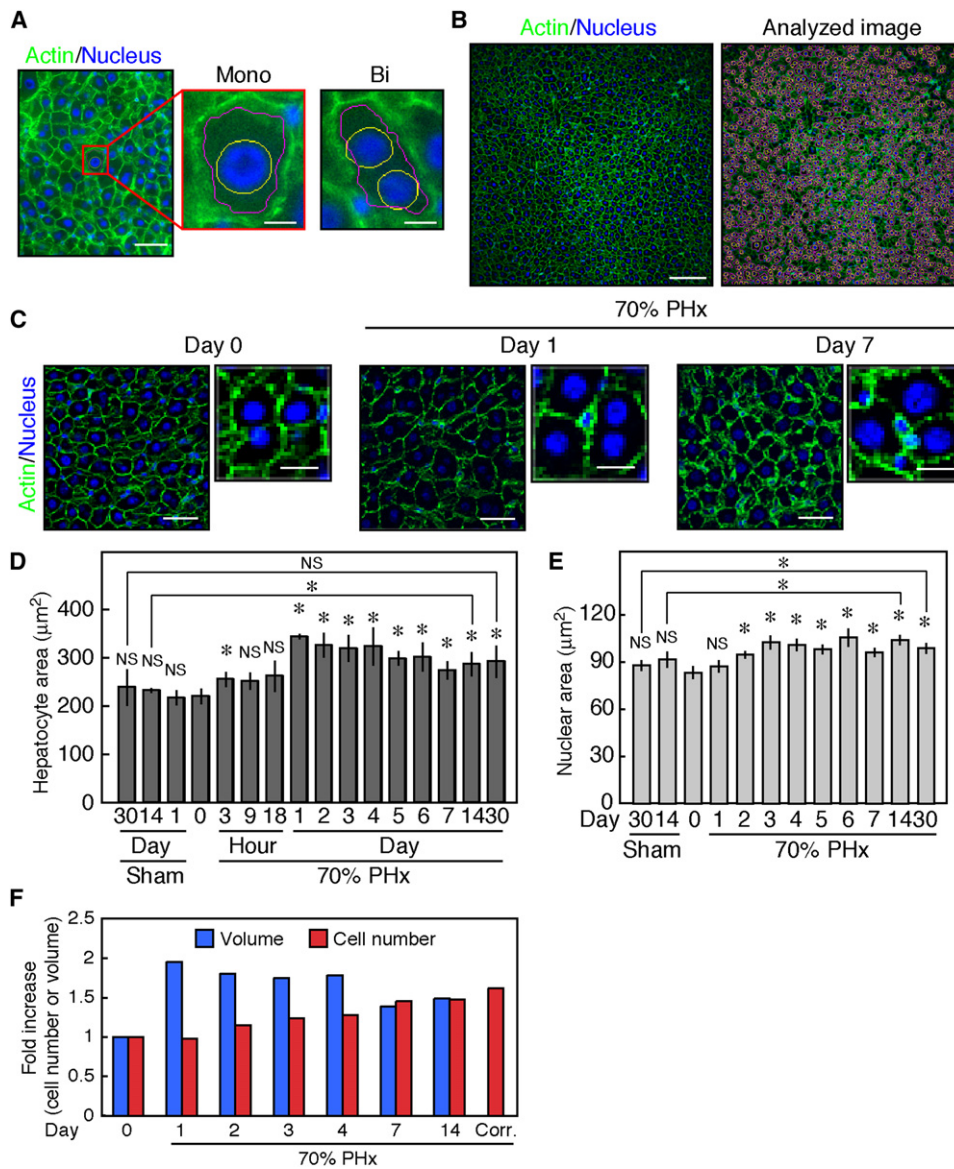
Figure 2. Hypertrophy of Hepatocytes during Liver Regeneration

(A) Recognition of nuclei and outlines of hepatocytes by imaging cytometry. Nuclei (blue) and actin (green) of hepatocytes were stained by Hoechst33342 and Phalloidin, respectively, in liver sections. The cytometer recognized nuclei (yellow) and outlines (magenta) of hepatocytes to calculate sectional area. This procedure also distinguishes mononuclear hepatocytes (Mono) from binuclear hepatocytes (Bi) and calculates their sectional area. Scale bars represent 25 μm for the left picture and 5 μm for the central and right pictures.

(B) An example of the analysis of liver sections by imaging cytometry. Actin (green) and nuclei (blue) staining allowed for the recognition of hepatocytes in liver sections. Scale bar represents 100 μm.

(C) The size of hepatocytes and their nuclei before and after 70% PHx. Actin (green) and nuclei (blue) staining showed hypertrophy of hepatocytes and their nuclei after 70% PHx. Note that hepatocytes increased their size whereas their nuclear size was not changed at day 1. Scale bars represent 25 μm for the larger photos and 12.5 μm for the smaller photos.

(D) Quantification of the size of hepatocytes during liver regeneration by imaging cytometry. The size of hepatocytes peaked at 1 day after 70% PHx and decreased thereafter. p values between each time point and day 0, and sham controls and the regenerated livers were calculated by Student's t test (*p < 0.05; NS, p > 0.05). Error bars represent SD.

(E) Quantification of the nuclear size of hepatocytes during regeneration after 70% PHx by imaging cytometry. The nuclear size increased after 70% PHx. p values between each time point and day 0, and sham controls and the regenerated livers were calculated by Student's t test (*p < 0.01; NS, p > 0.05). Error bars represent SD.

(F) Fold-increases in the volume and number of hepatocytes during liver regeneration. The values before PHx are set at 1. The volume was obtained by converting the sectional area of hepatocytes shown in (D), and the number was calculated from the quantified data on the labeled clusters of hepatocytes shown in Figure 3F. The fold-increase in the cell number 14 days after 70% PHx was corrected by the data obtained by serial section analysis (Figures 3G and 3H) and is also shown (Corr.). In the early phase, the liver regenerates almost entirely via hypertrophy. In the late phase, both hypertrophy and proliferation contribute to the regeneration.

but not the long-term hypertrophy. Furthermore, there was no remarkable change in organelles of hepatocytes in the regenerated liver (Figure S2B). Therefore, the density of hepatocytes before and after 70% PHx appears to be similar and the increase in liver weight is likely to reflect the increase in cell size.
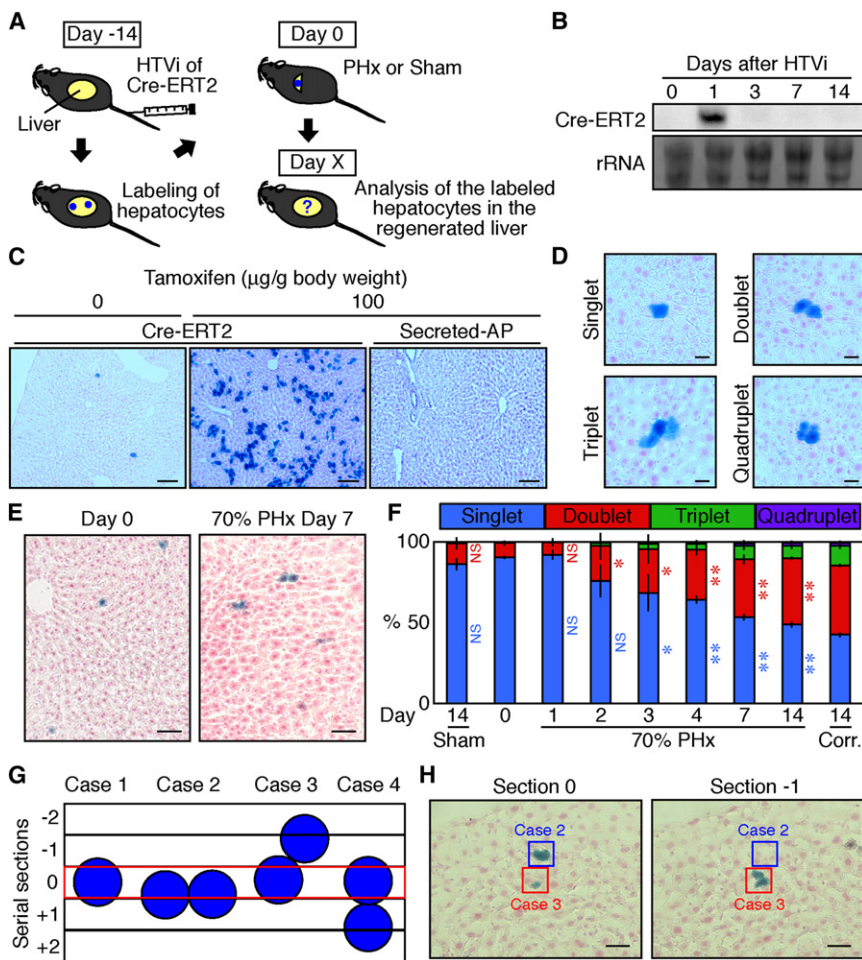
Figure 3. Genetic Labeling of Single Hepatocytes to Trace Cell Division

(A) Experimental scheme. The Cre-ERT2 expression vector was introduced into R26R mice by HTVi and DNA recombination was induced in hepatocytes. LacZ staining detected those hepatocytes that had undergone recombination. These mice were subjected to PHx or sham operation 14 days after HTVi and the LacZ+ hepatocytes were analyzed in the regenerated liver at various time points.

(B) Northern blot analysis of expression of Cre-ERT2 after HTVi. rRNA was used as the loading control.

(C) Genetic labeling of hepatocytes. LacZ staining of liver sections 14 days after HTVi showed that administration of tamoxifen 3 days after HTVi of the Cre-ERT2 expression vector induced DNA recombination at a high frequency. DNA recombination did not occur at all on expression of secreted alkaline phosphatase (Secreted-AP) even in the presence of tamoxifen. Without tamoxifen, expression of Cre-ERT2 resulted in DNA recombination in a few hepatocytes. Scale bars represent 100 μm.

(D) Neighboring labeled hepatocytes observed in the regenerated liver. We defined clusters comprising one, two, three, and four LacZ+ hepatocytes as singlets, doublets, triplets, and quadruplets, respectively. Scale bars represent 25 μm.

(E) LacZ staining of liver sections before and after 70% PHx. Before PHx (day 0), most labeled hepatocytes were singlets, whereas many doublets were observed 7 days after 70% PHx. Scale bars represent 50 μm.

(F) Quantification of the labeled clusters. Doublets increased from 2 days after 70% PHx. At 14 days after 70% PHx, about half of hepatocytes remained singlets. p values between each time point and day 0 for proportions of singlet (blue) and doublet (red) were calculated by

Student's t test (*p < 0.05; **p < 0.0005; NS, p > 0.05). Those p values between the regenerated liver and the sham control at day 14 were also statistically significant (p < 0.0005) though not indicated. The data at day 14 corrected by the serial section analysis are also shown (Corr.) Error bars represent SD.

(G) Schematic representation of the serial section analysis. We first observed and counted the number of the labeled clusters of hepatocytes on one section (colored by red and designated as 0). Then, we observed additional two serial sections both above and underneath the first section (designated as −2, −1, +1, and +2). In case 1 and case 2, we could correctly detect singlets and doublets at position 0, whereas it is difficult to distinguish between singlets and doublets aligning in z dimension like case 3 and case 4. However, in case 3, singlets and doublets can be distinguished by comparing at position 0 and −1. Because the diameter of hepatocytes is 20–30 μm and the thickness of the sections was 20 μm, the additional four sections were enough to determine the fraction of overlooked cells. Although this serial section analysis may not distinguish neighboring hepatocytes aligned completely vertically to the first sections, this case must be very rare (case 4).

(H) Examples of the serial section analysis. Examples of case 2 (blue square) and case 3 (red square) are shown. An apparent singlet on a section at 0 position was revealed to be a doublet on a section at −1 position in case 3. Scale bars represent 50 μm.

Genetic Single-Cell Labeling Shows Less than One Cell Division of Hepatocytes on Average during Liver Regeneration

To directly evaluate cell division, we developed a new procedure to genetically label a single hepatocyte using hydrodynamic tail vein injection (HTVi), an efficient means of delivering genes to hepatocytes [18]. We introduced the Cre-ERT2 vector by HTVi into Rosa26-LacZ reporter (R26R) mice to genetically label hepatocytes (Figure 3A). Northern blot analysis showed that Cre-ERT2 was strongly expressed just after HTVi, but the expression dropped markedly thereafter (Figure 3B). At 14 days after HTVi, the expression of Cre-ERT2 was no longer detected (Figure 3B), but a large number of hepatocytes expressed LacZ when tamoxifen was administered at 3 days after HTVi of Cre-ERT2 (Figure 3C). By contrast, HTVi of secreted alkaline phosphatase as a control induced no

recombination even in the presence of tamoxifen (Figure 3C). Unexpectedly, we noticed that HTVi of Cre-ERT2 did induce recombination even without tamoxifen in a few hepatocytes (Figure 3C). This tamoxifen-independent recombination was probably because of the strong transient expression of Cre-ERT2 in a few cells (Figure 3B). To trace each labeled cell, we utilized this low-frequency labeling without tamoxifen and performed PHx or a sham operation 14 days after HTVi, because the expression of Cre-ERT2 had vanished by that time (Figure 3B). There was no difference in liver regeneration between mice with and without HTVi, indicating that the liver had recovered from the damages, if any, caused by HTVi. Because hepatocytes exhibit different characteristics depending on the location in the liver lobule [21], we examined the location of the labeled hepatocytes and found that the genetic labeling occurred randomly throughout the lobule
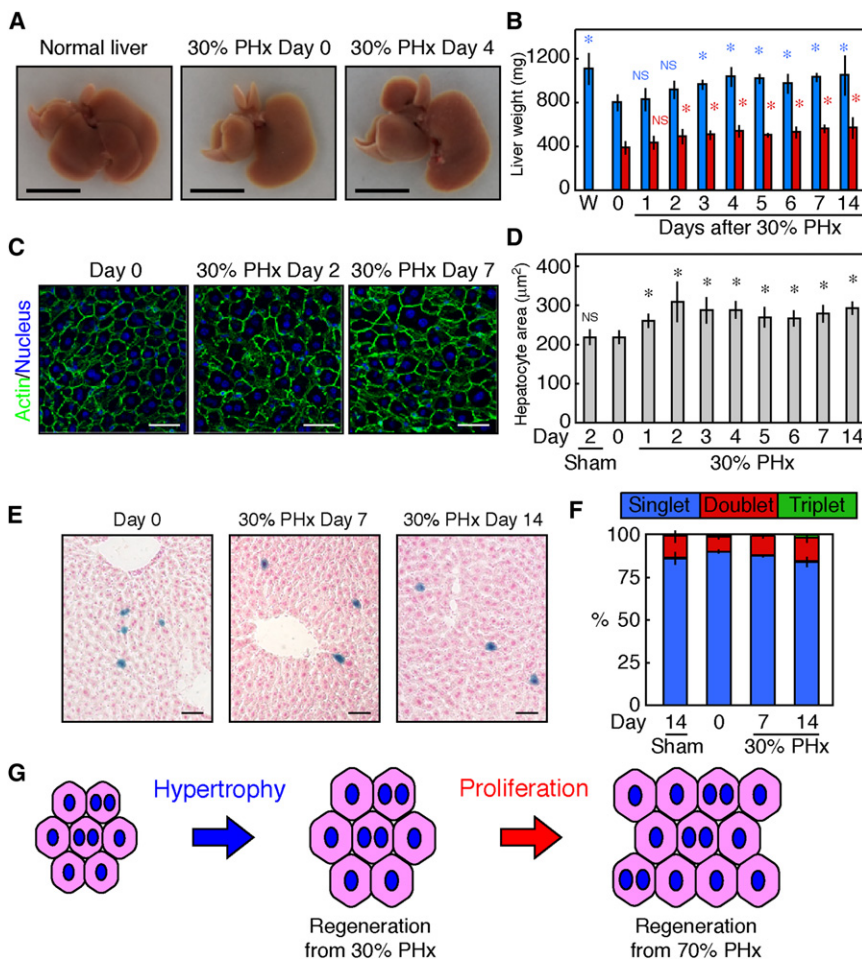
Figure 4. Cellular Hypertrophy and Cell Division of Hepatocytes after 30% PHx

(A) 30% PHx. In 30% PHx, the median lobe was surgically removed. The remaining lobes expanded by 4 days after 30% PHx. Scale bars represent 1 cm.

(B) Liver weight at different time points after 30% PHx. Because we analyzed right and caudate lobes in 70% PHx, we also analyzed them in 30% PHx. Thus, we separately weighed different lobes. Blue bars show weights of liver as a whole including all left, right, and caudate lobes, whereas red bars show those of only right and caudate lobes. p value between each time point and day 0 was calculated by Student's t test (*p < 0.05; NS, p > 0.1). Error bars represent SD.

(C) Images of hepatocytes after 30% PHx. Staining of actin (green) and nuclei (blue) showed that hepatocytes enlarged at 2 and 7 days after 30% PHx. Scale bars represent 25 μm.

(D) Quantification of the size of hepatocytes during liver regeneration after 30% PHx by imaging cytometry. p value between each time point and day 0 was calculated by Student's t test (*p < 0.05; NS, p > 0.9). Error bars represent SD.

(E) LacZ staining of hepatocytes after 30% PHx in the hepatocyte-labeling assay. Most of the LacZ+ hepatocytes observed after 30% PHx remained as singlets. Scale bars represent 50 μm.

(F) Quantification of the labeled clusters. Proportions of singlet and doublet were almost the same between the regenerated liver at day 14 and the sham control (p > 0.4 by Student's t test), indicating that hepatocytes rarely underwent cell division after 30% PHx. Error bars represent SD.

(G) A model of liver regeneration. In the first response to the loss of liver mass, hepatocytes enlarge, which is sufficient for the loss of 30% mass. In the case of 70% PHx, hypertrophy is not sufficient, and hepatocytes proliferate to increase the cell number.

(Figure S3). We performed 70% PHx on these mice with the labeled hepatocytes and found clusters comprising various numbers of the labeled cells. We defined clusters of one, two, three, and four hepatocytes as singlets, doublets, triplets, and quadruplets, respectively (Figure 3D). Clusters comprising more than five hepatocytes were very rare in all the conditions examined (see below). If a singlet underwent one cell division during liver regeneration, it should become a doublet. Therefore, the cell division of individual hepatocytes during liver regeneration can be traced. We counted the numbers of labeled clusters at various time points during liver regeneration. Before PHx, most of the labeled hepatocytes were singlets, whereas a considerable number of doublets were observed at 7 days after 70% PHx (Figure 3E). Consistent with the Ki67 staining (Figure 1C), doublets started to significantly increase from 2 days after 70% PHx, and about a half of the labeled clusters were doublets at 14 days after PHx. Triplets and quadruplets also emerged, though their numbers were small. Interestingly, a considerable proportion of the labeled cells remained as singlets, suggesting that not all the hepatocytes undergo cell division during regeneration (Figure 3F). A possible problem of this analysis is, however, potential overlooking of neighboring hepatocytes aligned in z dimension, especially in regenerated livers where about half of the labeled cells had undergone cell division (Figure 3G). To address this possibility, we performed serial section analysis of the liver 14 days after 70% PHx. In addition to the

section we first observed, we analyzed four additional serial sections to determine whether singlets in the first section are real singlets or doublets (Figures 3G and 3H). By this analysis, out of 93 apparent singlets, 9 turned out to be doublets and 3 were triplets, and out of 28 apparent doublets, 2 were triplets (Figure 3H and data not shown). With these values we corrected the data of 14 days after 70% PHx (Figure 3F). Even after the corrections, more than 42% of the labeled cells still remained as singlets. These results demonstrated that the number of hepatocytes increased by 1.6-fold during liver regeneration, which corresponded to an average of 0.7 cell division per cell (Figure 2F). As hepatocytes increased their volume by 1.5-fold (Figures 2D and 2F), the increases in the size and number of hepatocytes together (1.5 × 1.6 = 2.4-fold) would account for the 2.4-fold increase in liver weight (Figure 1B). Our results provide the first quantitative data on the size and number of hepatocytes during liver regeneration and evidence that not only proliferation but also cellular hypertrophy roughly equally contributes to regeneration.

Liver Regenerates from 30% PHx by Hypertrophy of Hepatocytes without Proliferation

To address whether the proliferation and hypertrophy make similar contributions to all the regenerative processes, we next analyzed liver regeneration after 30% PHx (Figure 4A). Liver weight increased from 1 day after 30% PHx and reached a plateau by 4 days (Figures 4A and 4B). The right and caudate

lobes, which also remain after 70% PHx, showed slightly greater increases in weight than the left lobe, as the remaining whole lobes increased in weight by 1.3-fold, whereas that of the right and caudate lobes alone increased by 1.5-fold (Figure 4B). As we analyzed the right lobe after 70% PHx, we also analyzed it after 30% PHx. Ki67 staining showed that a few hepatocytes entered the cell cycle from 2 days after 30% PHx (Figure S4A). Next, we investigated the size of hepatocytes by imaging cytometry. Actin staining showed hypertrophy of hepatocytes after 30% PHx (Figure 4C). Quantification revealed that the hepatocytes were largest at 2 days after 30% PHx and gradually decreased their size but remained larger than before 30% PHx (Figure 4D). Imaging cytometry showed slight, but not statistically significant, increase in nuclear size after 30% PHx (Figures S4B and S4C). We also observed that ploidy of hepatocytes showed only marginal increase after 30% PHx, in clear contrast to significant increase in ploidy after 70% PHx (Figure S4D). These results indicate that the hypertrophy of hepatocytes is independent of DNA content. We observed ultrastructures of hepatocytes after 30% PHx and found no remarkable difference in organelles similarly to after 70% PHx (Figure S2B). Hepatocytes had increased their size by 1.4-fold by 7 days after 30% PHx, which was almost equal to the 1.5-fold increase in the weight of the right and caudate lobes, suggesting that cellular hypertrophy alone compensated the lost tissue (Figures 4B and 4D). This possibility was further confirmed by the hepatocyte-labeling assay, i.e., hepatocytes rarely conducted cell division after 30% PHx (Figures 4E and 4F). These results clearly show that the liver regenerates from 30% PHx by increasing the size of hepatocytes without cell division.

Based on our findings, the general view of liver regeneration needs to be revised as discussed below. For regeneration from 30% PHx, hepatocyte hypertrophy is sufficient for the recovery. However, in a severe loss of liver mass such as 70% PHx, hypertrophy occurs first and cell division then follows to increase the cell number (Figure 4G).

Hepatocytes Infrequently Enter into M Phase during Liver Regeneration

Previous studies showed that a majority of hepatocytes were labeled by tritiated-thymidine [15]. We also found that more than 66% of hepatocytes incorporated BrdU by 3 days after 70% PHx (Figure S5A). Because some hepatocytes still entered the cell cycle thereafter (Figure 1C), and the labeling efficiency was not 100%, the actual population that entered S phase would be higher than 66%, confirming the previous observation. However, the incorporation of tritiated-thymidine or BrdU does not necessarily mean cell division of hepatocytes. Actually, we found that only about half of hepatocytes undergo cell division during liver regeneration (Figure 3F). We speculated that hepatocytes do enter into S phase but that there is a hurdle for them to enter into M phase.

To address this possibility, we developed a method to quantify the number of hepatocytes expressing a cell cycle marker in their nuclei by imaging cytometry (Figure S5B). We stained actin, a cell cycle marker (Ki67), and a mitosis marker (phosphorylated Histone H3 [pHH3]). We found that 48.9% and 21.9% of the cells were Ki67+ at 2 and 3 days after 70% PHx, respectively, whereas only 13.6% and 5.4% were pHH3+, respectively (Figures 1C, S5C, and S5E). For comparison, we examined the same markers in liver of postnatal day 10 (P10) mice, in which hepatocytes actively proliferate, and determined the ratio of pHH3+ cells to Ki67+ cells. The ratio was

significantly higher in the P10 mouse liver than the regenerating liver at 3 days after 70% PHx. The same tendency was observed at 2 days after 70% PHx (Figures S5D and S5F). These results support our idea that hepatocytes infrequently enter into M phase in regeneration compared to in liver development.

To further substantiate the existence of a hurdle for hepatocytes to enter into M phase, we investigated phosphorylation of Cdc (Cell division cycle) 2. Cdc2, a serine/threonine kinase, and Cyclin B form M phase promoting factor (MPF) that promotes the entry into M phase. The critical step to activate MPF is dephosphorylation of Cdc2 at Thr-14 and Tyr-15 [22]. In P10 liver, phosphorylation of Cdc2 at Tyr-15 was hardly detected. In sharp contrast, Cdc2 was strongly phosphorylated at Tyr-15 in regenerating liver 2 or 3 days after 70% PHx (Figure S5G). Therefore, the lower MPF activity in hepatocytes in regenerating liver might be a reason for the infrequent entry of hepatocytes into M phase.

Moreover, we observed that although there were some Ki67+ hepatocytes and more than 7% of hepatocytes were labeled by BrdU during liver regeneration from 30% PHx, they rarely underwent cell division (Figures 4E, 4F, S4A, and S5A). We also observed a significant increase in the nuclear size and ploidy of hepatocytes after liver regeneration after 70% PHx (Figures 2C, 2E, and S4D) as reported previously [14, 16]. Collectively, these results demonstrate that hepatocytes do enter S phase, but it is not always followed by normal M phase.

The Nuclear Number of Hepatocytes Decreases in Liver Regeneration

Despite the increase in ploidy of hepatocytes, the previous study by microscopic observation and manual counting showed that the number of nuclei in hepatocytes decreases during liver regeneration after 70% PHx [17]. Because our imaging cytometric approach is able to efficiently and objectively distinguish mononuclear and binuclear hepatocytes (Figure 2A), we investigated the nuclear number and confirmed that the proportion of binuclear hepatocytes decreased during liver regeneration after 70% PHx (Figures 5A and 5B). By contrast, it was unchanged during liver regeneration after 30% PHx (Figures 5A and 5B). The nuclear number of hepatocytes was reduced from 3 days after 70% PHx when the majority of hepatocytes had entered into the cell cycle (Figure 1C), whereas the nuclear number was constant during the regeneration after 30% PHx in which hepatocytes rarely divided (Figures 4E and 4F), suggesting a link between the reduction in the nuclear number and cell division.

To uncover this link, it is necessary to investigate individual hepatocytes. Therefore, we applied the single hepatocyte-labeling assay (Figure 3) with Nuclear Fast Red staining, which allowed us to determine the nuclear number in the genetically labeled hepatocytes (Figure 5C). As shown in Figure 3F, most of the labeled hepatocytes before PHx were singlets and about a half of them underwent cell division to become doublets (Figure 5D). Considering the nuclear number, there are three possible combinations of hepatocytes constituting doublets, i.e., two mononuclear hepatocytes, two binuclear hepatocytes, or a pair of mononuclear and binuclear hepatocytes (Figure 5D). Interestingly, however, the doublets that appeared 7 days after 70% PHx mostly consisted of two mononuclear cells, and no doublet with two binuclear cells was found (Figure 5E). Because most doublets were generated by cell division of singlets during liver regeneration, these results
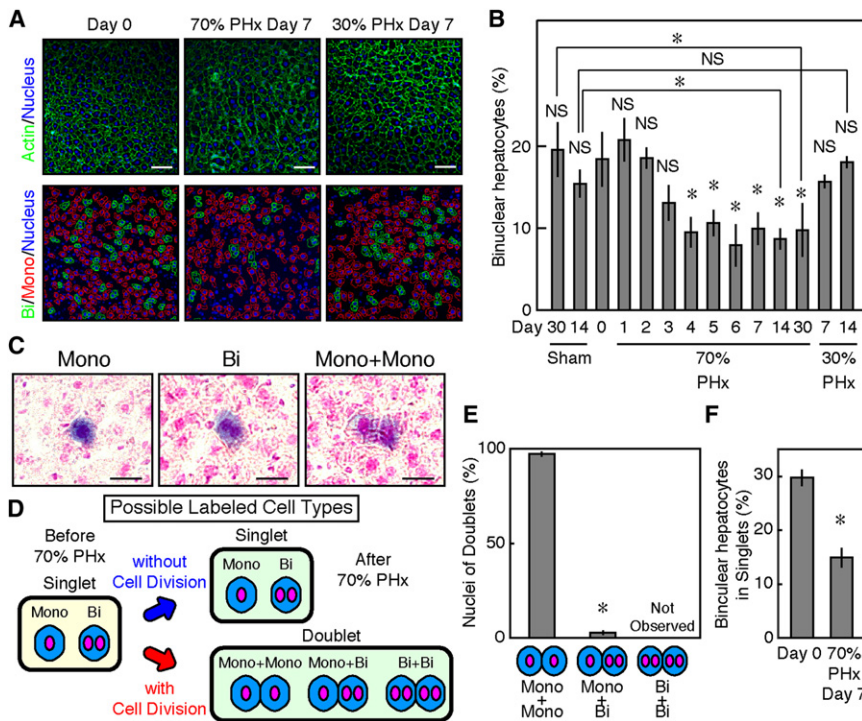
Figure 5. Relation between Cell Division and Nuclear Number during Liver Regeneration

(A) Mononuclear and binuclear hepatocytes. Staining of actin (green in the upper panel) and nuclei (blue in the upper panel) distinguishes mononuclear hepatocytes (Mono, red in the lower panel) from binuclear hepatocytes (Bi, green in the lower panel) by imaging cytometry. Note that the number of binuclear hepatocytes dropped 7 days after 70% PHx, but not after 30% PHx.

(B) Quantification of the proportion of binuclear hepatocytes during liver regeneration by imaging cytometry. p values between each time point and day 0, and sham controls and the regenerated livers were calculated by Student's t test ($*p < 0.05$; NS, $p > 0.05$). The proportion dropped markedly from 3 days after 70% PHx, but was constant after 30% PHx. Error bars represent SD.

(C) LacZ and Nuclear Fast Red staining of the labeled hepatocytes 7 days after 70% PHx. Nuclear Fast Red staining allowed us to count the nuclear number of the genetically labeled hepatocytes. Mono and Bi singlets and a Mono+Mono doublet are shown. Scale bars represent 25 μm.

(D) Possible labeled cell types after 70% PHx. Before PHx (day 0), most of the labeled hepatocytes are singlets with one nucleus (Mono) or two (Bi). During liver regeneration, about half of singlets remain as singlets without cell division and the other half undergo cell division to generate doublets. Thus, possible cell types 7 days after 70% PHx are singlets with one nucleus (Mono) or two nuclei (Bi) and doublets with either two Mono cells (Mono+Mono), two Bi cells (Bi+Bi), or a combination of Mono and Bi cells (Mono+Bi).

(E) Percentage of doublets with different combinations of Mono and Bi cells after 70% PHx. At least 50 doublets were counted per mouse. Most of the doublets comprised two Mono hepatocytes ($*p < 5 \times 10^{-8}$ by Student's t test). Doublets composed of two Bi hepatocytes were not observed. Error bars represent SD.

(F) Proportion of binuclear singlets in total singlets before and after 70% PHx. At least 100 singlets were counted per mouse. The proportion dropped after 70% PHx ($*p < 0.0005$ by Student's t test). Error bars represent SD.

indicated that cell division during liver regeneration mainly produced two mononuclear hepatocytes. Because about half of the singlets before PHx remained singlets without cell division after 70% PHx (Figures 3F and 5D), we also counted their nuclear number, and surprisingly found that the proportion of binuclear singlets in all singlets was reduced after the regeneration (Figure 5F). If both mononuclear and binuclear singlets undergo cell division at the same frequency to become doublets, the proportion of binuclear singlets in all remaining singlets after PHx should be constant. Instead, the proportion dropped significantly. One possible explanation for this observation is the preferential cell division of binuclear singlets to become doublets, though our results cannot exclude other possibilities such as nuclear fusion.

Modes of Mitosis in Binuclear Hepatocytes

To reveal how binuclear hepatocytes produce mononuclear cells, we analyzed each step of mitosis of hepatocytes during liver regeneration by examining the expression of Aurora B. Because the intracellular distribution of Aurora B changes markedly during cell division [23], distinct steps of mitosis can be identified by the localization of Aurora B and morphology of nuclei at 2 days after 70% PHx (Figure 6A). Although both mononuclear and binuclear hepatocytes were frequently observed in prophase, 205 out of 643 hepatocytes in prophase were binuclear, binuclear hepatocytes were very rare in prometaphase/metaphase, and only 3 of 154 hepatocytes were binuclear (Figure 6A). Furthermore, in anaphase, all 52 hepatocytes observed exhibited the segregation of two nuclei to each pole at opposite sides (Figure 6A). These results

indicate that condensed chromosomes gather at the center of both mononuclear and binuclear hepatocytes in prometaphase/metaphase and the two nuclei are segregated to two opposite poles in anaphase, resulting in apparently the same mode of prometaphase/metaphase and anaphase for both mononuclear and binuclear hepatocytes. In telophase, we observed mainly two neighboring mononuclear hepatocytes (178 out of 191) and a few pairs comprising a mononuclear hepatocyte and a binuclear hepatocyte (13 out of 191) (Figure 6A). Those daughter pairs with one mononuclear cell and one binuclear cell might be generated by occasional splitting of the condensed chromosomes derived from binuclear hepatocytes in one of the two daughter cells, similar to the observations in a recent report [24]. However, no pair of binuclear hepatocytes was found. The proportion of pairs in telophase was almost the same as that obtained by the single hepatocyte-labeling assay, confirming that cell division during liver regeneration mainly produced mononuclear hepatocytes (Figures 5F and S6).

It has been well established that hepatocytes often undergo mitosis without cytokinesis in liver development, generating binuclear hepatocytes [17, 25]. In liver regeneration, our results demonstrate that not all hepatocytes undergo M phase. Mononuclear hepatocytes that have entered into M phase produce two mononuclear hepatocytes via a conventional cell cycle. In contrast, binuclear hepatocytes that have entered into M phase assemble all condensed chromosomes from two nuclei and produce two mononuclear hepatocytes. Overall, the number of binuclear hepatocytes decreases during liver regeneration in contrast to liver development (Figure 6B).
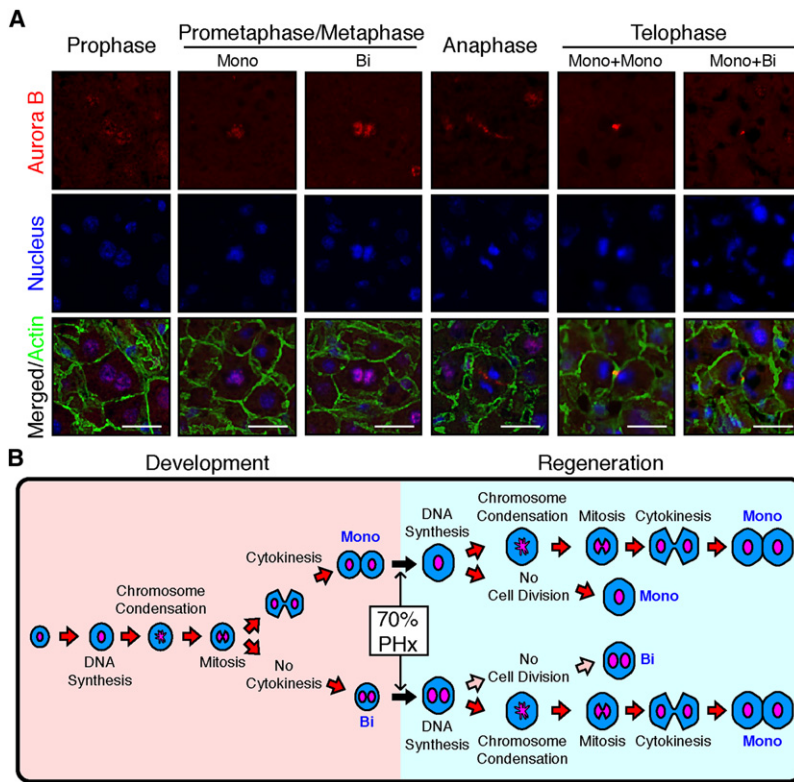
Figure 6. Cell Division of Hepatocytes during Liver Regeneration

(A) Modes of mitosis. We visualized the expression and localization of Aurora B (red) as well as actin (green) and nuclei (blue) by immunofluorescent staining. Prophase, prometaphase/metaphase, anaphase, and telophase were distinguished by the distribution of Aurora B and morphology of nuclei in liver sections at 2 days after 70% PHx. Mono and Bi hepatocytes and pairs of hepatocytes, Mono+Mono and Mono+Bi, were observed in prometaphase/metaphase and in telophase, respectively. Scale bars represent 20 μm.

(B) Modes of cell cycle during liver development and regeneration. In liver development, most Mono hepatocytes undergo the conventional cell cycle to replicate. However, some of them undergo mitosis without cytokinesis to produce Bi hepatocytes. During liver regeneration after 70% PHx, Mono hepatocytes remain without mitosis or undergo conventional mitosis and cytokinesis to replicate. Bi hepatocytes remain without mitosis or undergo cell division. In this cell division, condensed chromosomes from the two nuclei gather at the center of the hepatocyte in metaphase, and the nuclei are segregated to two poles to produce two Mono hepatocytes. Overall, these processes increase the number of Mono hepatocytes in the regenerated liver. Hepatocytes increase in size during both development and regeneration, whereas changes in nuclear number clearly differ between development and regeneration.

Discussion

Although hepatocytes are metabolically active, they are dormant in the cell cycle under normal conditions. In response to loss of liver mass, however, hepatocytes enter the cell cycle and regenerate the liver. A number of previous studies indicated that almost all hepatocytes proliferate after 70% PHx. However, we demonstrate that cellular hypertrophy significantly contributes to liver regeneration (Figure 4G). Moreover, we show that hepatocytes undergo cell division only about 0.7 times on average in the regeneration from 70% PHx (Figure 3). Our results are a significant contrast to previous studies and this difference is probably because of the experimental designs. Most of the previous studies were conducted on whole liver or bulk hepatocytes, whereas the current study employed two novel systems to examine individual hepatocytes: an imaging cytometric analysis and a genetic tracing system using HTVi.

Imaging cytometry enables an unbiased, objective, and high-throughput analysis of the size of hepatocytes (Figure 2). Furthermore, modification of this procedure allows analyses of the expression of cell cycle markers and of the number and size of nuclei of hepatocytes at the same time (Figures 2E, 5A, 5B, S5B, and S5E). To trace the fate of individual hepatocytes, we developed a novel genetic approach, in which a small population of hepatocytes can be permanently and randomly labeled at the single-cell level. If a labeled hepatocyte undergoes one cell division, the two daughter hepatocytes are expected to be next to each other. Thus, this procedure makes it possible to quantitatively analyze the cell division of individual hepatocytes (Figure 3).

We revealed that the early phase of liver regeneration from 70% PHx totally depends on the hypertrophy of hepatocytes (Figures 1B, 1C, 2C, 2D, and 2F). In addition, liver regeneration after 30% PHx is achieved solely by hypertrophy (Figure 4). Although hypertrophy of hepatocytes during liver regeneration has been considered to occur only when proliferative potential of hepatocytes is compromised, e.g., inhibition of cell cycle by genetic mutations [12, 14, 26] or administration of dexamethasone [27], our results indicate that hypertrophy of hepatocytes is the first process by which liver regenerates. Interestingly, expression of a significant number of genes is similarly up- or downregulated after both 30% and 70% PHx [28]. Therefore, it is likely that those genes contribute to the hypertrophy of hepatocytes after both 30% and 70% PHx. We speculate that the increase of liver mass by hypertrophy rather than cell division allows hepatocytes to respond to the immediate requirement to maintain homeostasis. Intriguingly, the very early stage of liver regeneration (0–4 hr after PHx in mice) is known as the "priming" phase, in which hepatocytes dramatically change their gene expression to respond to regenerative stimuli such as cytokines [29, 30]. Therefore, we speculate that this priming also triggers hypertrophy of hepatocytes. The facts that hypertrophy starts as early as 3 hr after 70% PHx (Figure 2D) and that 30% PHx induces both the priming and hypertrophy of hepatocytes further support our idea [31, 32].

We extensively investigated the cell cycle progression of hepatocytes during liver regeneration. Most hepatocytes entered S phase after 70% PHx (Figure S5A), consistent with previous reports [15, 33]. Interestingly, however, staining of pHH3 showed that only a small portion of hepatocytes entered M phase compared to that at P10 when hepatocytes actively proliferate, implying that some hepatocytes fail to enter M phase (Figures S5C–S5F). These observations could be simply due to longer interphase in liver regeneration than in liver development. However, it seems unlikely, because Cdc2 is

strongly phosphorylated at Tyr-15 only in regeneration (Figure S5G). Moreover, even though more than 7% of hepatocytes undergo S phase, hepatocytes rarely undergo cell division after 30% PHx (Figures 4E, 4F, and S5A). Thus it is more likely that there is a hurdle for hepatocytes to enter M phase during regeneration, leading to the infrequent cell division and increase in ploidy (Figure S4D).

As reported previously [17], we also found a reduction in binuclear hepatocytes during liver regeneration after 70% PHx (Figures 5A and 5B). The genetic labeling with nuclear staining of single hepatocytes and staining of Aurora B revealed that they undergo cell division to produce mononuclear hepatocytes (Figures 5E and 6A), which could occur more frequently for binuclear hepatocytes than for mononuclear ones (Figure 5F). This mode of cell division of binuclear hepatocytes has been previously reported in cultured hepatocytes [34]. Our results provide strong evidence for this type of cell division in vivo. Hepatocytes increase in number and size during both the development and regeneration of the liver, but cell cycle regulation differs significantly as shown in Figure 6B.

A long-standing question is why liver can regenerate. Although to a lesser extent, some organs other than liver also increase their size in response to partial loss. For example, the removal of one kidney induces the enlargement of the other. In this case, kidney cells rarely intake BrdU, implying that the kidney increases in size through cellular hypertrophy [35], similar to after 30% PHx (Figure S5A). Therefore, cellular hypertrophy may be a general mechanism to compensate for the partial loss of an organ. However, the liver can recover even from a 70% loss caused by PHx, and this extraordinary potential to regenerate may be due to the unique capacity of hepatocytes for both hypertrophy and proliferation. Interestingly, hepatocytes under normal conditions and after 30% and 70% PHx show significant differences in cell number, cell size, nuclear number, nuclear size, and ploidy. Nevertheless, livers under these different conditions still maintain homeostasis, indicating a "cellular robustness" of hepatocytes to perform their required functions. A recent report on the extreme plasticity of ploidy through cell division also supports the robustness of hepatocytes [24, 36]. Furthermore, as mentioned above, hepatocytes deficient in either Skp2, Stat3, or Separase markedly increased their size after 70% PHx to maintain almost normal liver functions despite the altered cell cycle progression [12, 14, 26], supporting this notion. This cellular robustness seems to be unique to hepatocytes and may be a reason why the liver has an extremely high capacity to regenerate.

Although liver regeneration has been studied extensively, fundamental questions as to the cell division cycle of hepatocytes have remained largely unanswered. This study has uncovered the importance of hypertrophy and unique features of hepatocytes in the progression of the cell cycle during regeneration and revises the currently accepted view on liver regeneration after surgical resection.

Experimental Procedures

Statistical Analysis
All the data represented in graphs are averages ± SD. For measurement of liver weight, three to seven mice were sampled per each condition. For other experiments, three mice were analyzed per each condition.

Mice
All the mice used in this study were the C57BL/6 background. Rosa26-LacZ reporter (R26R) mice were purchased from the Jackson Laboratory. Both 30% and 70% PHx were performed on 8-week-old male mice in all the experiments. All experimental procedures in this study were approved by the institutional animal care and use committee of the University of Tokyo.

Genetic Labeling of Hepatocytes
We used the pLIVE vector and *Trans*IT-EE Hydrodynamic Delivery Solution (Mirus Bio) to introduce cDNAs into R26R mice by hydrodynamic tail vein injection (HTVi).

Imaging Cytometry
We used IN Cell Analyzer 2000 (GE Healthcare). Hoechst33342, Alexa Fluor 488 phalloidin, and antibodies against markers for the cell cycle gave signals for nuclei, cellular outlines, and the expression levels of the markers, respectively.

Northern and Western Blot Analyses
The methods used for the northern and western blot analyses were described previously [37].

Supplemental Information

Supplemental Information includes Supplemental Experimental Procedures and six figures and can be found with this article online at doi:10.1016/j.cub.2012.05.016.

References

1. Conlon, I., and Raff, M. (1999). Size control in animal development. Cell *96*, 235–244.
2. Lui, J.C., and Baron, J. (2011). Mechanisms limiting body growth in mammals. Endocr. Rev. *32*, 422–440.
3. Fankhauser, G. (1945). Maintenance of normal structure in heteroploid salamander larvae, through compensation of changes in cell size by adjustment of cell number and cell shape. J. Exp. Zool. *100*, 445–455.
4. Henery, C.C., Bard, J.B., and Kaufman, M.H. (1992). Tetraploidy in mice, embryonic cell number, and the grain of the developmental map. Dev. Biol. *152*, 233–241.
5. Neufeld, T.P., de la Cruz, A.F., Johnston, L.A., and Edgar, B.A. (1998). Coordination of growth and cell division in the *Drosophila* wing. Cell *93*, 1183–1193.
6. Savage, V.M., Allen, A.P., Brown, J.H., Gillooly, J.F., Herman, A.B., Woodruff, W.H., and West, G.B. (2007). Scaling of number, size, and metabolic rate of cells with body size in mammals. Proc. Natl. Acad. Sci. USA *104*, 4718–4723.
7. Michalopoulos, G.K. (2007). Liver regeneration. J. Cell. Physiol. *213*, 286–300.
8. Michalopoulos, G.K., and DeFrances, M. (2005). Liver regeneration. Adv. Biochem. Eng. Biotechnol. *93*, 101–134.
9. Si-Tayeb, K., Lemaigre, F.P., and Duncan, S.A. (2010). Organogenesis and development of the liver. Dev. Cell *18*, 175–189.
10. Alison, M.R., Islam, S., and Lim, S. (2009). Stem cells in liver regeneration, fibrosis and cancer: the good, the bad and the ugly. J. Pathol. *217*, 282–298.
11. Palmes, D., and Spiegel, H.U. (2004). Animal models of liver regeneration. Biomaterials *25*, 1601–1611.
12. Haga, S., Ogawa, W., Inoue, H., Terui, K., Ogino, T., Igarashi, R., Takeda, K., Akira, S., Enosawa, S., Furukawa, H., et al. (2005). Compensatory

recovery of liver mass by Akt-mediated hepatocellular hypertrophy in liver-specific STAT3-deficient mice. J. Hepatol. *43*, 799–807.

13. Haga, S., Ozaki, M., Inoue, H., Okamoto, Y., Ogawa, W., Takeda, K., Akira, S., and Todo, S. (2009). The survival pathways phosphatidylinositol-3 kinase (PI3-K)/phosphoinositide-dependent protein kinase 1 (PDK1)/Akt modulate liver regeneration through hepatocyte size rather than proliferation. Hepatology *49*, 204–214.

14. Minamishima, Y.A., Nakayama, K., and Nakayama, K. (2002). Recovery of liver mass without proliferation of hepatocytes after partial hepatectomy in Skp2-deficient mice. Cancer Res. *62*, 995–999.

15. Grisham, J.W. (1962). A morphologic study of deoxyribonucleic acid synthesis and cell proliferation in regenerating rat liver; autoradiography with thymidine-H3. Cancer Res. *22*, 842–849.

16. Satyanarayana, A., Wiemann, S.U., Buer, J., Lauber, J., Dittmar, K.E.J., Wüstefeld, T., Blasco, M.A., Manns, M.P., and Rudolph, K.L. (2003). Telomere shortening impairs organ regeneration by inhibiting cell cycle re-entry of a subpopulation of cells. EMBO J. *22*, 4003–4013.

17. Gerlyng, P., Abyholm, A., Grotmol, T., Erikstein, B., Huitfeldt, H.S., Stokke, T., and Seglen, P.O. (1993). Binucleation and polyploidization patterns in developmental and regenerative rat liver growth. Cell Prolif. *26*, 557–565.

18. Herweijer, H., and Wolff, J.A. (2007). Gene therapy progress and prospects: hydrodynamic gene delivery. Gene Ther. *14*, 99–107.

19. Ding, B.S., Nolan, D.J., Butler, J.M., James, D., Babazadeh, A.O., Rosenwaks, Z., Mittal, V., Kobayashi, H., Shido, K., Lyden, D., et al. (2010). Inductive angiocrine signals from sinusoidal endothelium are required for liver regeneration. Nature *468*, 310–315.

20. Shteyer, E., Liao, Y., Muglia, L.J., Hruz, P.W., and Rudnick, D.A. (2004). Disruption of hepatic adipogenesis is associated with impaired liver regeneration in mice. Hepatology *40*, 1322–1332.

21. Kaestner, K.H. (2009). In the zone: how a hepatocyte knows where it is. Gastroenterology *137*, 425–427.

22. Norbury, C., Blow, J., and Nurse, P. (1991). Regulatory phosphorylation of the p34cdc2 protein kinase in vertebrates. EMBO J. *10*, 3321–3329.

23. Ruchaud, S., Carmena, M., and Earnshaw, W.C. (2007). Chromosomal passengers: conducting cell division. Nat. Rev. Mol. Cell Biol. *8*, 798–812.

24. Duncan, A.W., Taylor, M.H., Hickey, R.D., Hanlon Newell, A.E., Lenzi, M.L., Olson, S.B., Finegold, M.J., and Grompe, M. (2010). The ploidy conveyor of mature hepatocytes as a source of genetic variation. Nature *467*, 707–710.

25. Margall-Ducos, G., Celton-Morizur, S., Couton, D., Brégerie, O., and Desdouets, C. (2007). Liver tetraploidization is controlled by a new process of incomplete cytokinesis. J. Cell Sci. *120*, 3633–3639.

26. Wirth, K.G., Wutz, G., Kudo, N.R., Desdouets, C., Zetterberg, A., Taghybeeglu, S., Seznec, J., Ducos, G.M., Ricci, R., Firnberg, N., et al. (2006). Separase: a universal trigger for sister chromatid disjunction but not chromosome cycle progression. J. Cell Biol. *172*, 847–860.

27. Nagy, P., Teramoto, T., Factor, V.M., Sanchez, A., Schnur, J., Paku, S., and Thorgeirsson, S.S. (2001). Reconstitution of liver mass via cellular hypertrophy in the rat. Hepatology *33*, 339–345.

28. Li, J., Campbell, J.S., Mitchell, C., McMahan, R.S., Yu, X., Riehle, K.J., Bumgarner, R.E., and Fausto, N. (2009). Relationships between deficits in tissue mass and transcriptional programs after partial hepatectomy in mice. Am. J. Pathol. *175*, 947–957.

29. Fausto, N. (2000). Liver regeneration. J. Hepatol. *32* (1, Suppl), 19–31.

30. Su, A.I., Guidotti, L.G., Pezacki, J.P., Chisari, F.V., and Schultz, P.G. (2002). Gene expression during the priming phase of liver regeneration after partial hepatectomy in mice. Proc. Natl. Acad. Sci. USA *99*, 11181–11186.

31. Webber, E.M., Godowski, P.J., and Fausto, N. (1994). In vivo response of hepatocytes to growth factors requires an initial priming stimulus. Hepatology *19*, 489–497.

32. Mitchell, C., Nivison, M., Jackson, L.F., Fox, R., Lee, D.C., Campbell, J.S., and Fausto, N. (2005). Heparin-binding epidermal growth factor-like growth factor links hepatocyte priming with cell cycle progression during liver regeneration. J. Biol. Chem. *280*, 2562–2568.

33. Bucher, N.L., and Swaffield, M.N. (1964). The rate of incorporation of labeled thymidine into the deoxyribonucleic acid of regenerating rat liver in relation to the amount of liver excised. Cancer Res. *24*, 1611–1625.

34. Guidotti, J.E., Brégerie, O., Robert, A., Debey, P., Brechot, C., and Desdouets, C. (2003). Liver cell polyploidization: a pivotal role for binuclear hepatocytes. J. Biol. Chem. *278*, 19095–19101.

35. Liu, B., and Preisig, P.A. (2002). Compensatory renal hypertrophy is mediated by a cell cycle-dependent mechanism. Kidney Int. *62*, 1650–1658.

36. Duncan, A.W., Hanlon Newell, A.E., Smith, L., Wilson, E.M., Olson, S.B., Thayer, M.J., Strom, S.C., and Grompe, M. (2012). Frequent aneuploidy among normal human hepatocytes. Gastroenterology *142*, 25–28.

37. Miyaoka, Y., Tanaka, M., Naiki, T., and Miyajima, A. (2006). Oncostatin M inhibits adipogenesis through the RAS/ERK and STAT5 signaling pathways. J. Biol. Chem. *281*, 37913–37920.